



Supplement of

HONO chemistry at a suburban site during the EXPLORE-YRD campaign in 2018: formation mechanisms and impacts on O₃ production

Can Ye et al.

Correspondence to: Keding Lu (k.lu@pku.edu.cn) and Yuanhang Zhang (yhzhang@pku.edu.cn)

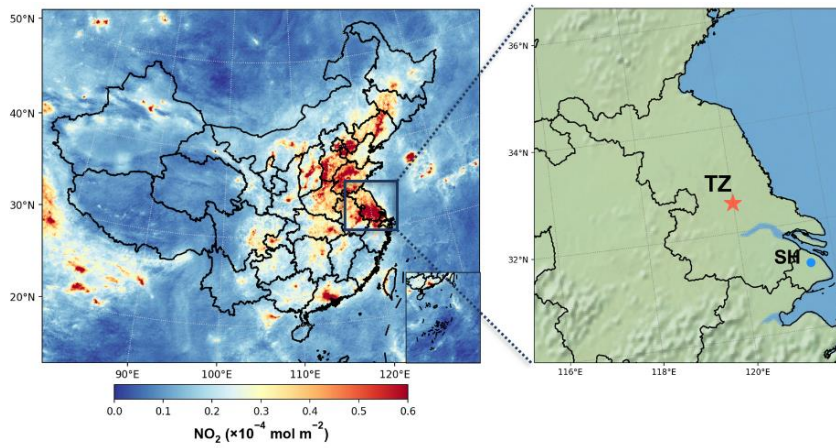
The copyright of individual parts of the supplement might differ from the article licence.

35 **Table S1:** Measured parameters and corresponding measurement techniques

Parameters	Limit of detection	Methods	Accuracy
HONO	5 ppt	LOPAP	±10%
OH	$6 \times 10^5 \text{ cm}^{-3}$	LIF	±10%
NO	60 ppt	Chemiluminescence	±20%
NO ₂	0.3 ppb	Chemiluminescence+ Photolytic converter	±20%
O ₃	0.5 ppb	UV photometry	±5%
CO	1 ppb	Infrared absorption	±1 ppb
SO ₂	0.1 ppb	Pulsed UV fluorescence	±5%
S _a	14-700 nm	SMPS	±20%
HCHO	25 ppt	Hantzsch fluorimetry	±5%
VOCs	20-300 ppt	GC-FID/MS	±15%
PM _{2.5}	$0.1 \mu\text{g m}^{-3}$	TEOM	±5%
NH ₄ ⁺ , SO ₄ ²⁻ , NO ₃ ⁻ , Cl ⁻	$0.05 \mu\text{g m}^{-3}$	GAC-IC	±20%

40

45



50

Figure S1: Location of the field measurement site (red star) in Taizhou (TZ), Jiangsu Province. This site is situated approximately 200 km northwest of Shanghai (SH), one megacity in YRD. The left map is colored by monthly average NO₂ column density (July, 2018) retrieved from TROPOMI (<https://s5phub.copernicus.eu/dhus>).

55

60

65

70

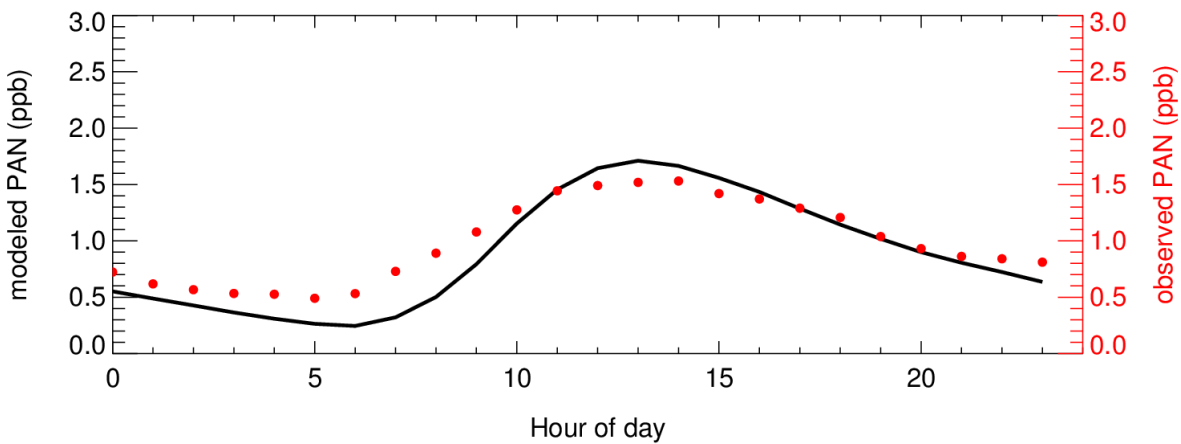


Figure S2: Averaged diurnal pattern of observed and modeled PAN if A first-order dilution loss term with a lifetime of 8 hours was incorporated.

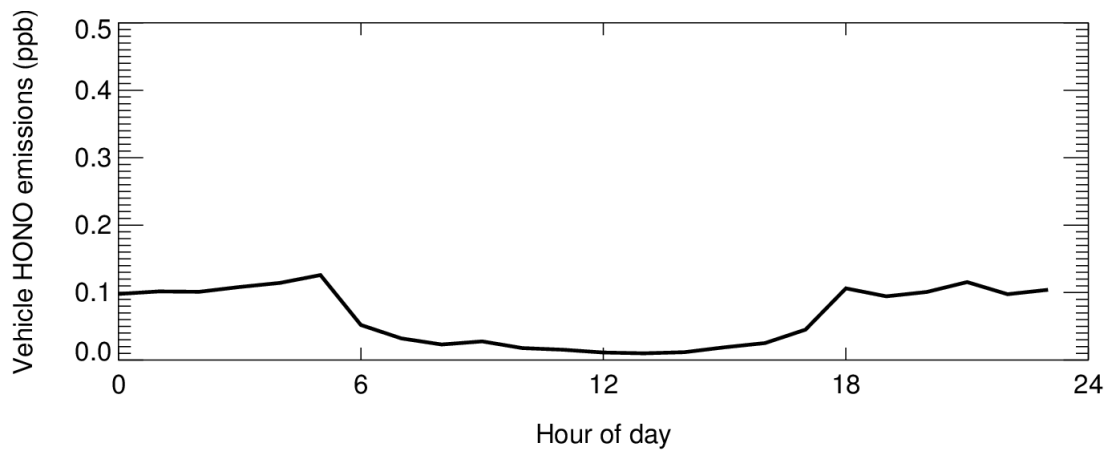


Figure S3: Calculated HONO diurnal profile contributed by vehicle emissions.

95

100

105

110

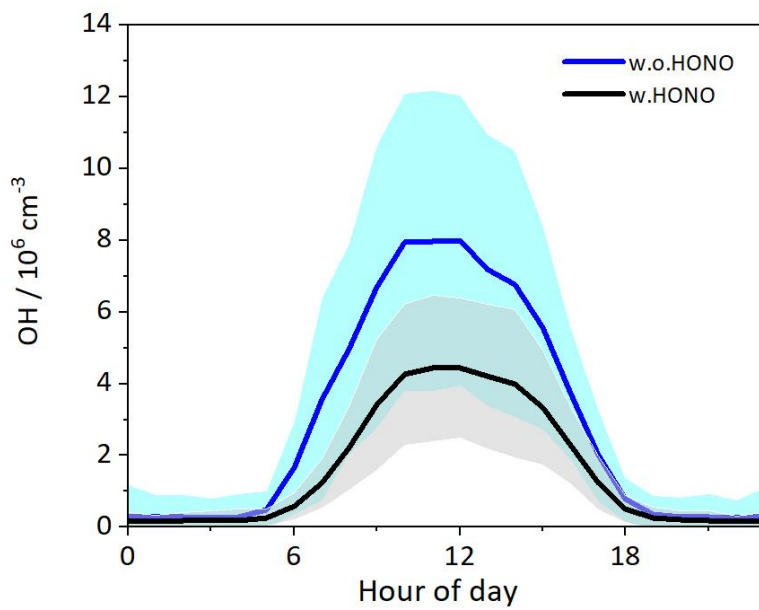


Figure S4: The comparison of modeled OH concentration with and without observed HONO as a model constraint.